European Conference on Optical Communication (ECOC) 2022 © Optica Publishing Group 2022

Ultra-wideband All-optical Interband Wavelength Conversion Using a Low-complexity Dispersion-engineered SOI Waveguide

Isaac Sackey[(1)], Gregor Ronniger[(1)], Carsten Schmidt-Langhorst[(1)], Robert Elschner[(1)], Md Mahasin Khan[(1)], Hidenobu Muranaka[(2)], Tomoyuki Kato[(2)], Shun Okada[(2)], Tsuyoshi Yamamoto[(2)], Yu Tanaka[(2)], Takeshi Hoshida[(2)], Colja Schubert[(1)], and Ronald Freund[(1)]

[(1)] Fraunhofer Institute for Telecommunications, HHI, Einsteinufer 37, 10587 Berlin, Germany (Email: isaac.sackey@hhi.fraunhofer.de)

[(2)] Fujitsu Ltd, 4-1-1 Kamikodanaka, Nakahara-ku, Kawasaki 211-8588, Japan

Abstract *We experimentally present a low-complexity dispersion-engineered all-optical wavelength-converter using a photonic integrated-circuit based on SOI waveguide. We achieve a single-sided conversion bandwidth of ~35 nm from C- to S-band, and successfully transmit a converted 1-channel 32-GBd single-polarization QPSK S-band data over a 100-km SSMF link. ©2022 The Author(s)*

Introduction

Increased capacity of optical networks is a key requirement in a wide range of applications (e.g. media streaming, cloud computing or industry automation). One way of satisfying this demand is using multi-band transmission systems [1,2]. However, proper equipment for generation of high fidelity data signals is not always available outside the C-band. Therefore, a promising approach is to make use of existing components and use all-optical wavelength conversion (AOWC) to translate those signals from the C-band to other bands of interest. With the potential of converting a whole band at once, the all-optical approach is cost- and power-efficient as the effort quickly amortizes with increasing number of channels. AOWC is transparent to modulation format and symbol rate, which is in stark contrast to typical electronic domain implementations.

Particularly, the use of AOWC based on integrated waveguides has drawn much attention in recent years due to their high nonlinear coefficient, small footprint and their ability for photonic integration [3-6]. To improve the performance of planar waveguide based AOWC, several approaches have been reported [5,7,8].

In this paper, we focus on optimizing the performance of a low-complexity AOWC using a cost-effective standard 220-nm Silicon-on-Insulator (SOI) technology. We demonstrate its capabilities by converting 32 GBd QPSK signals from C- to S-band and observed an optical signal-to-noise ratio (OSNR) penalty of < 0.3 dB. Furthermore, we successfully transmitted the converted S-band signal over a 100-km link of standard single-mode fiber (SSMF).

Experimental setup

Fig. 1(a) represents the experimental setup used for investigation of 32 GBd single-polarization QPSK data (S- and C-band) under back-to-back (b2b) conditions, while the setup in Fig. 1(b) is used for performance evaluation of the converted S-band signal after noise-loading, and after transmission over a 100-km SSMF link.

To generate a reference for OSNR degradation evaluations, a continuous wave (CW) signal emitted by a tuneable external cavity laser (ECL), capable of providing S- and C-band light, was modulated by a commercially available C-band $LiNbO_3$ IQ-modulator to yield a 32 GBd single-polarization QPSK data as shown in Fig. 1(a). The variable optical attenuator (VOA) in front of the Erbium-doped fiber amplifier (EDFA) was adjusted to sweep the received OSNR. We used a wavelength selective switch (WSS) to suppress the out-of-band amplified spontaneous

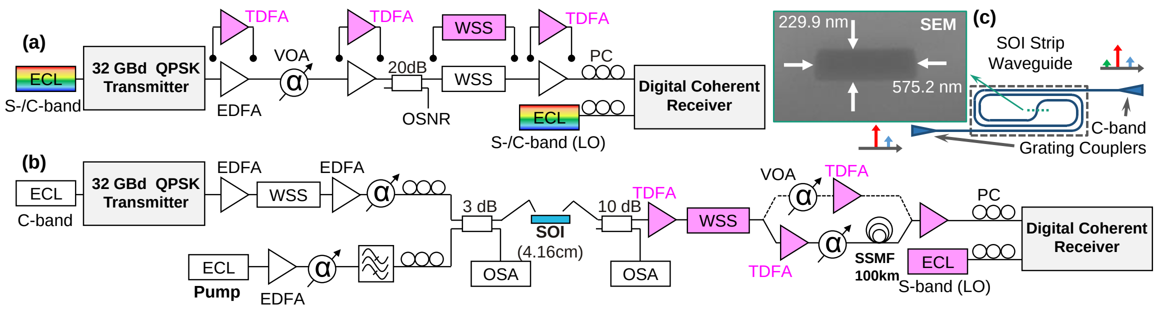

Fig. 1: Experimental setups: (a) back-to-back for noise loading measurements of either C-band data only or S-band data only using a commercially available C-band transceiver. (b) Transmission of a converted 32 GBd QPSK signal over a 100-km SSMF link, and for noise loading measurement of the wavelength converter. (c) SEM image and schematic of PIC layout.

emission (ASE) noise. In order to perform the OSNR reference measurements for S-band data signals, the EDFAs and the C-band WSS were replaced by S-band devices (e.g. Thulium-doped fiber amplifier (TDFA)) as depicted in Fig. 1(a). We employed a commercially available C-band digital coherent receiver for the reception of both C-band and S-band data signals.

Fig. 1(b) shows the all-optical photonic integrated circuit (PIC)-based C- to S-band wavelength converter in both a back-to-back and a transmission testbed. In the realization, we combined the C-band data signal and a pump wave at 1530 nm using a 3 dB optical coupler. One of the outputs of the coupler served as an input optical light to a 4.16 cm SOI spiral waveguide via a grating coupler, whereas the other output of the 3 dB coupler served as a monitor port to an optical spectrum analyser (OSA). Note: the waveguide cross sectional scanning electron microscopy (SEM) image and a schematic of the layout is shown in Fig. 1(c). The VOAs on both the pump and the data signal paths enabled control of the optical powers into the SOI waveguide. Parametric process through four-wave mixing (FWM) in the waveguide yielded S-band data signals. After amplifying the output signals of the SOI waveguide, a WSS was used to select the desired S-band data signals before performance evaluation was performed on the converted S-band signals after the data was sent through a noise-loading stage or over a 100-km SSMF transmission link. The pre-amplified C-band coherent receiver consisted of a local oscillator (LO, 100-kHz linewidth), a 90° optical hybrid, a pair of balanced photodetectors, and a two-channel real-time oscilloscope (80 GS/s, 32 GHz). Offline digital signal processing was then performed, including resampling, data-aided channel estimation, frequency-domain MIMO equalization, blind-phase-search carrier phase recovery, compensation of I/Q imbalances and phase errors, de-mapping and bit-error counting.

Results and Discussions

To properly characterize the interband AOWC, saturation characteristics of the device were initially evaluated. Firstly, the data signal was turned off and the pump input power to the SOI chip was adjusted from 0 dBm to +29.6 dBm. Note that the pump wavelength was kept at 1530 nm in our experiments. For each pump input power, the corresponding SOI output pump power was measured. Fig. 2(a) shows the pump saturation results. It can be seen that the pump saturates at input powers around +17.5 dBm. This observation is attributed to two-photon absorption (TPA) induced free-carrier absorption (FCA), and it is responsible for the increase in nonlinear losses of the waveguide. Nevertheless, low pump power requirement is a key factor for AOWC in our envisaged application. With the aim of achieving a low-complexity design, mechanisms to reduce the nonlinear loss of the waveguide such as p-i-n diode [7] were not implemented in our realization. The linear loss (including grating couplers) of our 4.16 cm waveguide was measured to be < 15 dB. In the signal saturation characteristic evaluation, two different pump input powers were investigated.

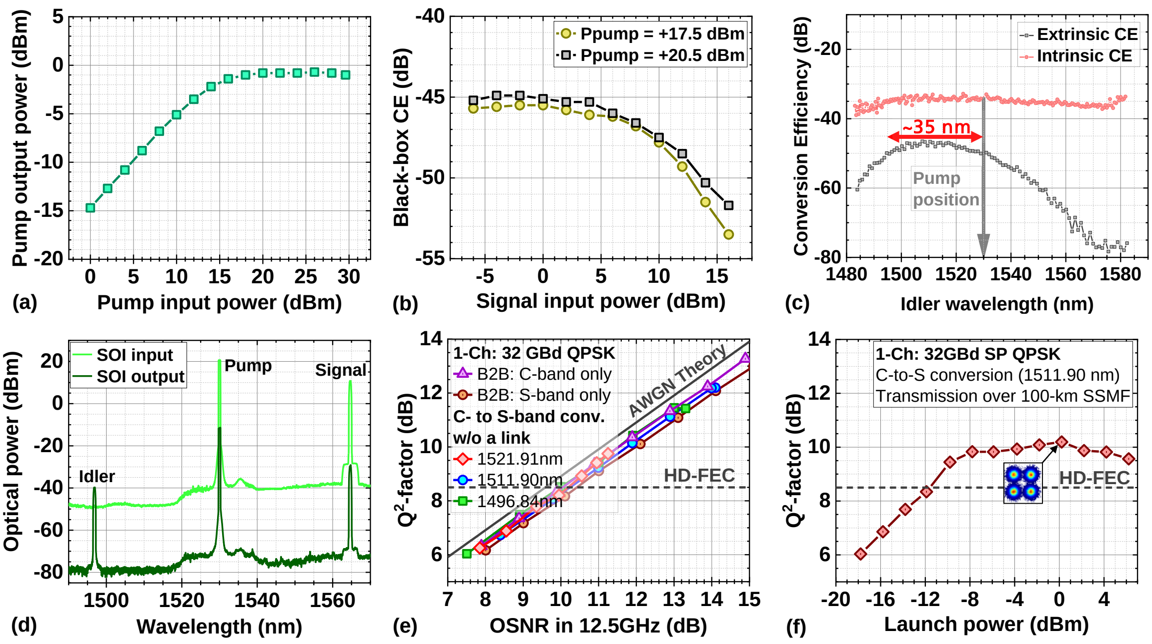

Fig. 2: Performance evaluation of the SOI-based interband wavelength converter: (a) Pump saturation characteristics, (b) Signal saturation characteristics for pump input powers of +17.5 dBm and +20.5 dBm, (c) Extrinsic and intrinsic idler CEs, (d) SOI input and output optical spectra at a resolution bandwidth of 0.5 nm, (e) b2b Q^2-factor vs OSNR measurements without a transmission link, (f) Q^2-factor performances of the generated S-band data over a 100-km SSMF transmission link.

Initially, the pump input power was set to +17.5 dBm and the input power of a CW signal (modulation turned off) was adjusted from -6 dBm to +16 dBm in steps of 2 dB. The wavelength of the signal was arbitrary set to 1548.32 nm. The black-box conversion efficiency (CE) for each signal input power was evaluated. We define CE as the ratio of the idler power (at the output of the waveguide) to the signal input power. Next, the investigations were repeated for a pump power of +20.5 dBm. Fig. 2(b) shows the summary of the signal saturation measurements. It can be deduced from the figure that beyond +5-dBm signal input power, the CE begins to saturate. Depleting the pump by the high signal input power leads to this nonlinear behaviour. Consistent with the measurements in Fig. 2(a), the increase in pump input power beyond +17.5 dBm did not significantly increase the CE performance as shown in Fig. 2(b).

Secondly, we evaluated the conversion bandwidth and the wavelength-dependent CE of the AOWC. In order to achieve an optimized idler power, the input and output grating coupler angles of the waveguide were skewed to optimize for C-band input and S-band output signals, respectively. At pump and signal input powers of +20.5 dBm and +5.7 dBm, respectively, the CW signal wavelength was swept from 1481 nm to 1579 nm and the corresponding idler CE values were calculated. We interpret this evaluated classical conversion efficiency as "*extrinsic"* because it includes the wavelength-dependent losses of the grating couplers. In order to evaluate the "*intrinsic*" CE, the grating coupler angles were set to the same value, and their wavelength-dependent loss values were de-embedded from the "extrinsic" CE measurement. We define the intrinsic CE as the ratio of idler power (at waveguide output) to the waveguide signal input power, evaluated without the losses of the grating couplers. It is evident from Fig. 2(c) that a 3 dB single-sided extrinsic conversion bandwidth (shown as black symbols) of ~35 nm is achievable with our dispersion-engineered SOI waveguide. Still better, the intrinsic conversion bandwidth (shown as red symbols) yielded a 3-dB bandwidth of more than 40 nm. The measured maximum extrinsic and intrinsic CEs were -46.5 dB and -32.8 dB, respectively. In Fig. 2(d), we exemplary show the optical spectra at the input and output of the PIC for a 32 GBd QPSK data signal (at 1564.68 nm) and its generated S-band idler.

Furthermore, we conducted OSNR reference measurements for both C-band and S-band data signals using a commercially available C-band transceiver (see Fig. 1(a)). The measured BERs were converted to Q^2-factors using the relation: $Q_{dB}^2 = 20 \times log_{10}\left[\sqrt{2}\, erfc^{-1}(2 \times BER)\right]$. As shown in Fig. 2(e), the OSNR implementation penalties of the 1-channel 32 GBd single-polarization QPSK C-band data and the S-band data, w.r.t. the additive white Gaussian noise (AWGN) theory at the hard-decision forward error correction (HD-FEC) threshold (BER = 3.8×10^{-3}, i.e. Q^2-factor = 8.5 dB), were found to be ~0.4 dB and 0.8 dB, respectively. The observed further degradation in the S-band data is attributed to the use of a C-band transceiver for the generation and reception of the S-band data. To properly quantify the performance of the AOWC, the transmitted data signal was independently set to three different wavelengths (1538.19 nm, 1548.52 nm, and 1564.68 nm). Using a signal and a pump input power of +10.8 dBm and +20.5 dBm, respectively, we evaluated the Q^2-factors of the generated S-band idlers (1521.91 nm, 1511.90 nm, and 1496.84 nm). The OSNR implementation penalties of the AOWC for all the investigated scenarios, w.r.t. the C-band b2b case at HD-FEC threshold, were found to be < 0.3 dB as shown in Fig. 2(e). The differences in the maximum OSNR of the idlers is due to non-uniform ASE profile of the used TDFA.

Finally, the AOWC was placed in a transmission testbed (see Fig. 1(b)). We transmitted the generated 1-channel S-band data, at a wavelength of 1511.90 nm, over a 100-km SSMF link. The launch power of the transmitted idler was adjusted from -16 dBm to +6 dBm. It can be seen from Fig. 2(f) that launch powers above -12 dBm provided Q^2-factors better than the HD-FEC threshold. The optimum launch power was found to be at 0 dBm.

Our fabricated AOWC is also capable of converting WDM signals and it is expected that the realization of a multiband system using a subsystem component such as our PIC-based AOWC will significantly increase the transmission capacity in a cost-effective fashion. However, it is expected that due to the flat dispersion characteristics required to achieve a wide conversion bandwidth, severe inter-channel crosstalk can be created. Thus, our future work will focus on WDM investigations.

Conclusions

We experimentally investigated the suitability of a low-complexity dispersion-engineered all-optical wavelength converter for future multi-band systems. We translated individual QPSK signals across the C-band to the S-band. Although it requires only a simple technology, the converter demonstrated a bandwidth of at least 35 nm, while only using 20.5-dBm pump power. Finally, a converted 32 GBd QPSK S-band signal was successfully transmitted over a 100-km SSMF.

References

[1] T. Kato, S. Watanabe, T. Yamauchi, G. Nakagawa, H. Muranaka, Y. Tanaka, Y. Akiyama, and T. Hoshida, "Real-time transmission of 240×200-Gb/s signal in S+C+L triple-band WDM without S- or L-band transceivers," in *Proc. Eur. Conf. on Opt. Commun., (ECOC)*, Dublin, Ireland, 2019, PDP, PD.1.7., DOI: 10.1049/cp.2019.1021

[2] I. Sackey, R. Elschner, R. Emmerich, C. Schmidt-Langhorst, D. D. Groß, G. Rademacher, Y. Awaji, H. Furukawa, T. Hasegawa, C. Schubert, and R. Freund, "Performance Evaluation of an Interband All-Optical Wavelength Converter for Cost-Effective High-Capacity Optical Networks," in *Proc. Eur. Conf. on Opt. Commun., (ECOC)*, Bordeaux, France, 2021, We4C1.5, DOI: 10.1109/ECOC52684.2021.9606078

[3] F. Da Ros, M. P. Yankov, E. P. da Silva, M. Pu, L. Ottaviano, H. Hu, E. Semenova, S. Forchhammer, D. Zibar, M. Galili, K. Yvind, and L. K. Oxenløwe, "Characterization and optimization of a high-efficiency AlGaAs-on-Insulator-based wavelength converter for 64- and 256-QAM signals," *J. Lightwave Technol.* Vol. 35, no. 17, pp. 3750–3757, 2017, DOI: 10.1109/JLT.2017.2722013

[4] D. T. H. Tan, K. Ikeda, P. C. Sun, and Y. Fainman, "Group velocity dispersion and self phase modulation in silicon nitride waveguides," *Appl. Phys. Lett.* Vol. 96, no. 6, p. 061101, 2010, DOI: 10.1063/1.3299008

[5] M. A. Foster, A. C. Turner, R. Salem, M. Lipson, and A. L. Geata, "Broad-band continuous-wave parametric wavelength conversion in silicon nanowaveguides," *Optics Express*, vol 15, no. 20, pp. 12949-12958, 2007, DOI: 10.1364/OE.15.012949

[6] T. Richter, R. Nouroozi, H. Suche, W. Sohler, and C. Schubert, "PPLN waveguide based tunable wavelength conversion of QAM data within the C-band," *IEEE Photon. Technol. Lett.*, vol. 25, no. 21, pp. 2085–2088, 2013, DOI: 10.1109/LPT.2013.2281464

[7] A. Gajda, L. Zimmermann, M. Jazayerifar, G. Winzer, H. Tian, R. Elschner, T. Richter, C. Schubert, B. Tillack, and K. Petermann, "Highly efficient CW parametric conversion at 1550 nm in SOI waveguides by reverse biased p-i-n junction," *Optics Express*, vol 20, no. 12, pp. 13100-13107, 2012, DOI: 10.1364/OE.20.013100

[8] G. Ronniger, I. Sackey, T. Kernetzky, U. Höfler, C. Mai, C. Schubert, N. Hanik, L. Zimmermann, R. Freund, and K. Petermann, "Efficient Ultra-Broadband C-to-O Band Converter Based on Multi-Mode Silicon-on-Insulator Waveguides," in *Proc. Eur. Conf. on Opt. Commun., (ECOC)*, Bordeaux, France, 2021, We1G.1, DOI: 10.1109/ECOC52684.2021.9606033